

N69-40323  
NASA-106310

Sixth Quarterly Progress Report  
(covering the period July 1 to September 30, 1969)

on


✓ NSR 22-009-288

A Study of Fluid Dynamics of Gaseous Nuclear Rockets

Work this quarter has been primarily concentrated on the empirical correlations of vortex data. The results of this study are contained in C. A. Rodoni's thesis (Ref. 1). The major results of his study are summarized in Appendix A. Rather than publish a report on this study at the present time, the information obtained from this study will be incorporated in the comprehensive review of the state of knowledge of vortex flows and how such flows relate to fluid dynamic containment which will constitute the final report on this contract. Copies of the thesis are available upon request.

October 1, 1969

CASE FILE  
COPY

  
W. S. Lewellen  
Project Supervisor

## Appendix A

### Summary of

#### An Investigation of the Flow Parameters of a Confined Turbulent Vortex

Carl Arthur Rodoni

In this study an attempt was made to find out to what extent empirically derived correction terms to laminar theories can be used successfully to predict turbulent results, and to look for direct correlations of the characteristic flow parameters in terms of the independent flow variables of the system.

A literature search was conducted to obtain the experimental data to be used in the correlations (see Ref. 2). A computer program was then written to find the optimum grouping of independent flow parameters which would fit the dependent parameters to a given curve.

Using this curve fitting method, empirical correlations were attempted for the ratio of the tangential velocity at the peripheral wall to the jet injection velocity ( $v_w/v_{jet}$ ), the ratio of the tangential to radial velocities ( $v/u$ ), the ratio of the circulation ( $\Gamma = vr$ ) at the radius of the exhaust hole to the circulation just outside of the peripheral wall boundary layer ( $\Gamma_e/\Gamma_{.8}$ ), the ratio of the circulation at the radius of the exhaust hole to the maximum achievable circulation ( $\Gamma_e/\Gamma_{ideal}$ ), the ratio of the mass flow through the vortex to the "no-swirl" mass flow ( $\bar{W}_0$ ), and the maximum tangential Mach number in the vortex ( $M_{t_{max}}$ ).

One of the best correlations achieved in this work was for the normalized mass flow ratio ( $\bar{W}_0$ ). The empirical correlation shown in Fig. 1 allows the prediction of the mass flow ratio  $\bar{W}_0$  for a vortex in terms of

the parameters  $r_e/r_o$ , the ratio of the exhaust hole radius to the outer wall radius;  $A_i/A_e$ , the ratio of inlet area to the exhaust area;  $L/D$ , the length-to-diameter ratio of the chamber; and  $N_H$ , the number of exhausts. It was found that  $\bar{W}_o$  was primarily a function of  $r_e/r_o$  and  $L/D$  for  $L/D > 2$  and primarily a function of  $r_e/r_o$ , only, when  $L/D < 2$ .

The momentum balance theory of Kendall and Roschke (Ref. 3) is also substantiated by the recovery factor data. The results shown in Figs. 2 and 3 show that correlations for the recovery factor can be obtained in terms of the momentum balance theory, within the range of the expected data scatter. According to these correlations,  $v_w/v_{jet}$  is primarily a function of the ratio of the injection area to the peripheral wall area ( $A_i/A_w$ ).

The effective skin friction coefficient for the peripheral wall has been shown to be larger than that predicted by the turbulent flat plate formula. (See Fig. 4). This increase in  $C_f$  is due to the presence of other dissipative factors in the flow such as turbulent shear terms, wall curvature, jet mixing, etc. The skin friction coefficient calculated over the chamber end-walls is also considerably higher than that predicted by turbulent flat plate results (Fig. 5).

The correlations shown in Figs. 6 and 7 show that the velocity ratio ( $v/u$ ) is a function of the parameters  $r_e/r_o$  and  $L/D$  as well as the area ratio  $A_i/A_w$  predicted by the momentum balance theory. The presence of these geometrical terms not predicted by the momentum balance theory tends to indicate the presence of other flow phenomena which the theory has ignored.

One explanation for the presence of the  $r_e/r_o$  and  $L/D$  terms as well as the increased dissipation observed in the vortices is a flow phenomenon which may be called "exhaust hole choking." This effect may be caused by the fact that when the fraction of the energy invested in the swirl is above a certain value, further increases in the swirl actually reduce the angular momentum which can pass through the exhaust holes (See Ref. 4). The flow then must rearrange itself to increase the level of dissipation and thus reduce the swirl at the exhaust.

The fact that the correlations presented for the ideal circulation ratio in Figures 8, 9 and 10 have much less data scatter than the recovery factor correlations in Figures 2 and 3 or the circulation ratio correlations of Figures 11 and 12 argues that the flow regions near the peripheral wall and in the center of the vortex are coupled in some manner.

The flow mechanism of "exhaust hole choking" not only accounts for this flow coupling, but also provides explanations for the observed parametric trends in the empirical correlations. The postulation of this "exhaust hole choking" effect would account for the deviation of the velocity ratio correlations of Fig. 6 and 7 from the values of  $v/u$  predicted by the momentum balance theory as well as the  $L/D$  dependence of  $C_f$  in Fig. 5.

Although, the correlations for the ideal circulation ratio appear to establish a definite flow dependence, the trends shown should be viewed with a certain amount of reservation. According to these correlations (shown in Figs. 8 and 9),  $\Gamma_e/\Gamma_{ideal}$  is a function of  $r_e/r_o$ ,  $A_i/A_w$ , and  $P_o/P_e$ . These correlations do have very little data scatter involved in them, but they also contain very few data points, and the pressure ratio

dependence shown in them may be valid over a limited range only. Therefore, the correlation shown in Fig. 10 is preferable to these, even though it has greater data scatter. This is because Fig. 10 contains more data points, and has a more reliable parameter dependence. According to this correlation  $\Gamma_e/\Gamma_{ideal}$  is a function of  $r_e/r_o$ ,  $A_i/A_w$ , and  $Re_t$ .

The differences between the theoretical curves and data points on Fig. 11 can be used to define an "effective eddy viscosity". Relatively small differences in circulation lead to large values of eddy viscosity as seen in Fig. 12.

The three-dimensional theory on which Fig. 12 is based (Ref. 5) checks out well with experimentally observed flow patterns. In Fig. 13, the values of the flow stagnation radius ( $\hat{r}/r_o$ ) as measured by Travers in Ref. 6 are shown to be in good agreement with the flow model predictions. Thus if the flow model breaks down, it must do so at some point inside the stagnation radius.

REFERENCES

1. Rodoni, Carl A., "An Investigation of the Flow Parameters of a Confined Turbulent Vortex," S. M. Thesis, Department of Aeronautics and Astronautics, M.I.T. (August, 1969).
2. Newton, W. H., "Correlations of Dissipation in Confined Turbulent Vortices," S. M. Thesis, Department of Aeronautics and Astronautics, M.I.T. (August, 1968).
3. Roschke, E. J., "Heat Transfer and Fluid Mechanics," California Institute of Technology, Jet Propulsion Laboratory, Space Programs Summary No. 37-20, Volume IV (1963).
4. Lewellen, W. S., Burns, W. J., and Strickland, H. J., "Transonic Swirling Flow," AIAA paper no. 68-693 (June 1968).
5. Rosenzweig, M. L., Lewellen, W. S., and Ross, D. H., "Confined Vortex Flows with Boundary Layer Interaction," Aerospace Corporation ATN-64(9227)-2 (1964).
6. Travers, A., "Experimental Investigation of Radial-Inflow Vortexes in Jet-Injection and Rotating-Peripheral-Wall Water Vortex Tubes," United Aircraft Research Laboratories Report F-910091-4, prepared under Contract No. NASw-847 (September 1967).
7. Keyes, J., Chang, T., and Sartory, W., "Hydromagnetic Stabilization of Jet Driven Vortex Flow," Oak Ridge National Laboratory Report ORNL-TM-1896 (October 1967).
8. Roschke, E. J., "Experimental Investigation of a Confined, Jet-Driven Water Vortex," California Institute of Technology, Jet Propulsion Laboratory, Technical Report No. 32-982 (October 1966).

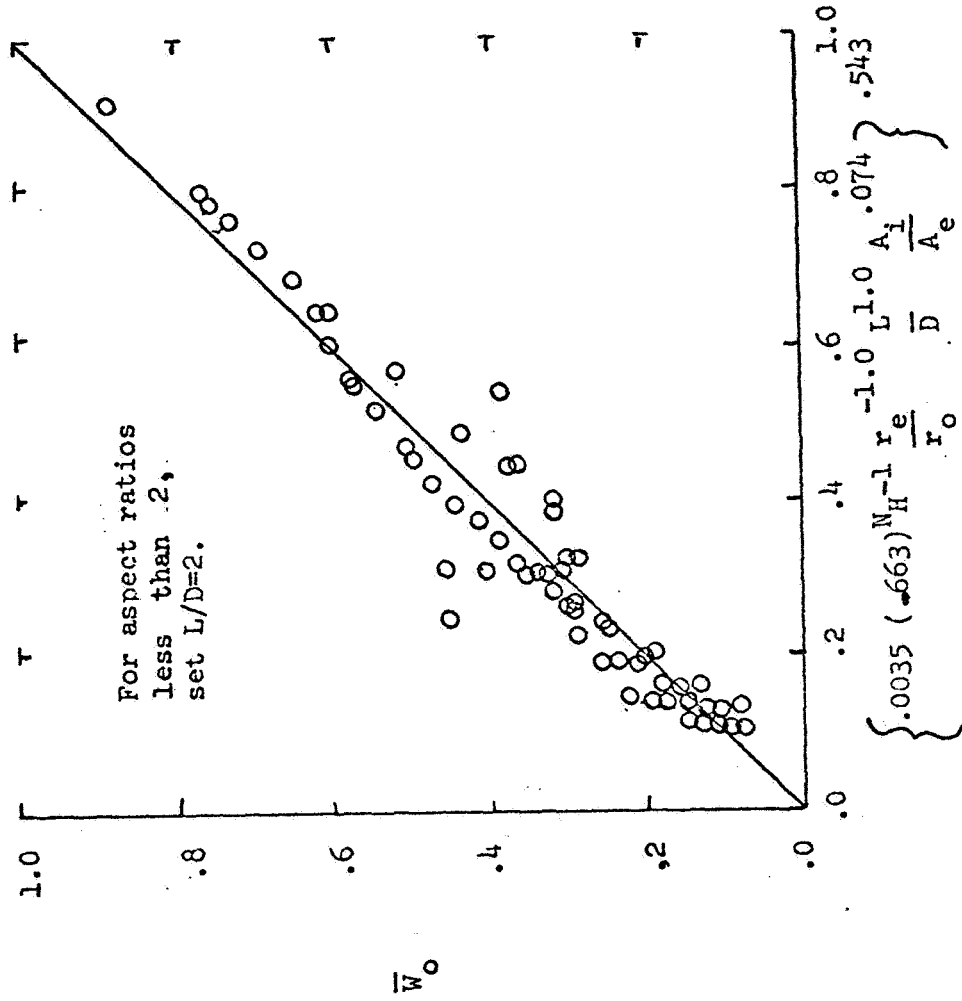


FIG. 1 The ratio of the mass flow through the vortex chamber to the "no-swirl" mass flow as a function of  $r/r_o$ , the ratio of the exhaust hole radius to the outer wall radius;  $A_i/A_e$ , the ratio of the inlet area to the exhaust area;  $L/D$ , the length-to-diameter ratio of the chamber and  $N_H$ , the number of exhausts.

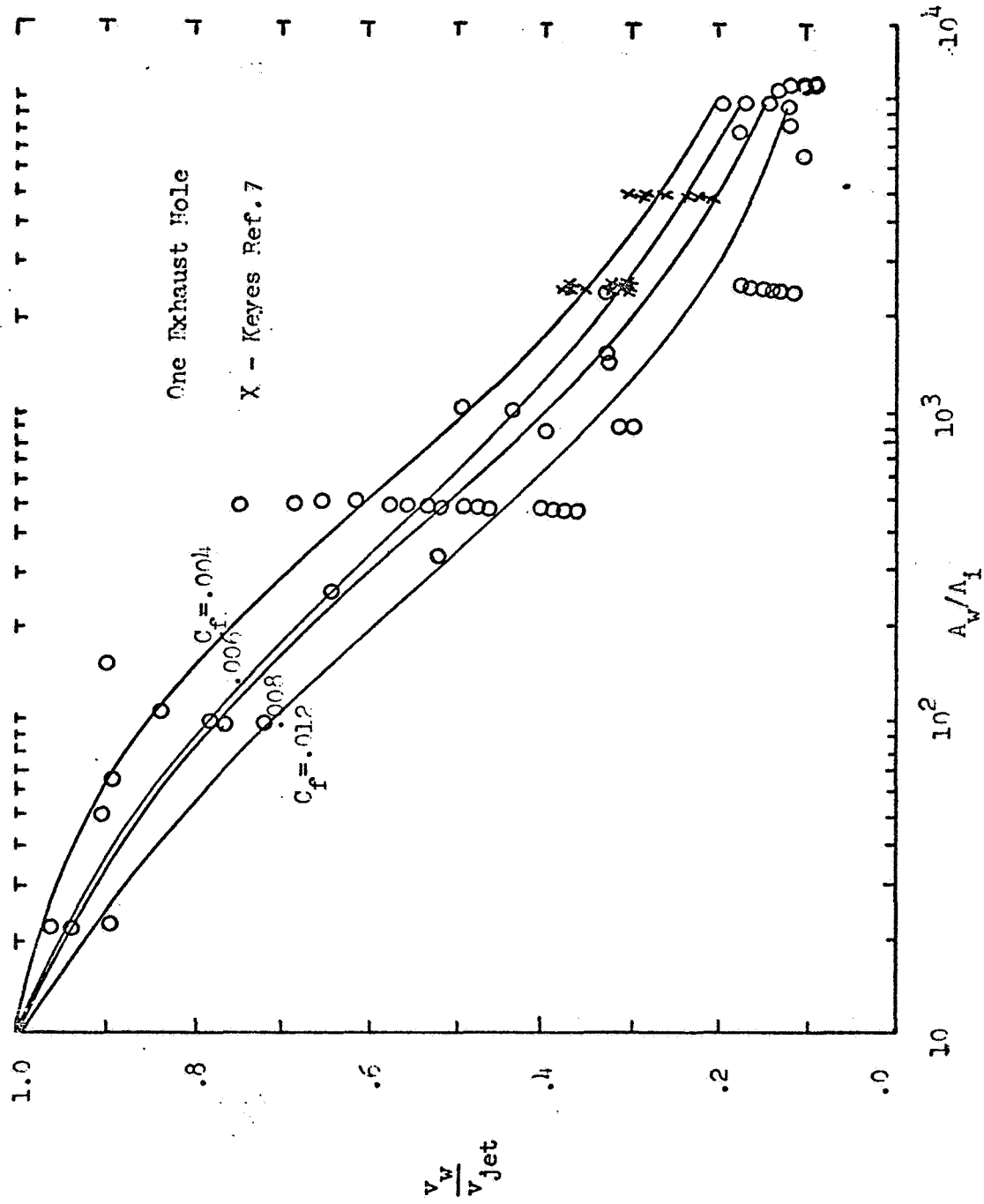


FIG. 2 The recovery factor  $V_w/V_{jet}$  as a function of  $A_w/A_1$ , the ratio of the peripheral wall area to the injection area, with the coefficient of friction  $C_f$  as a parameter.



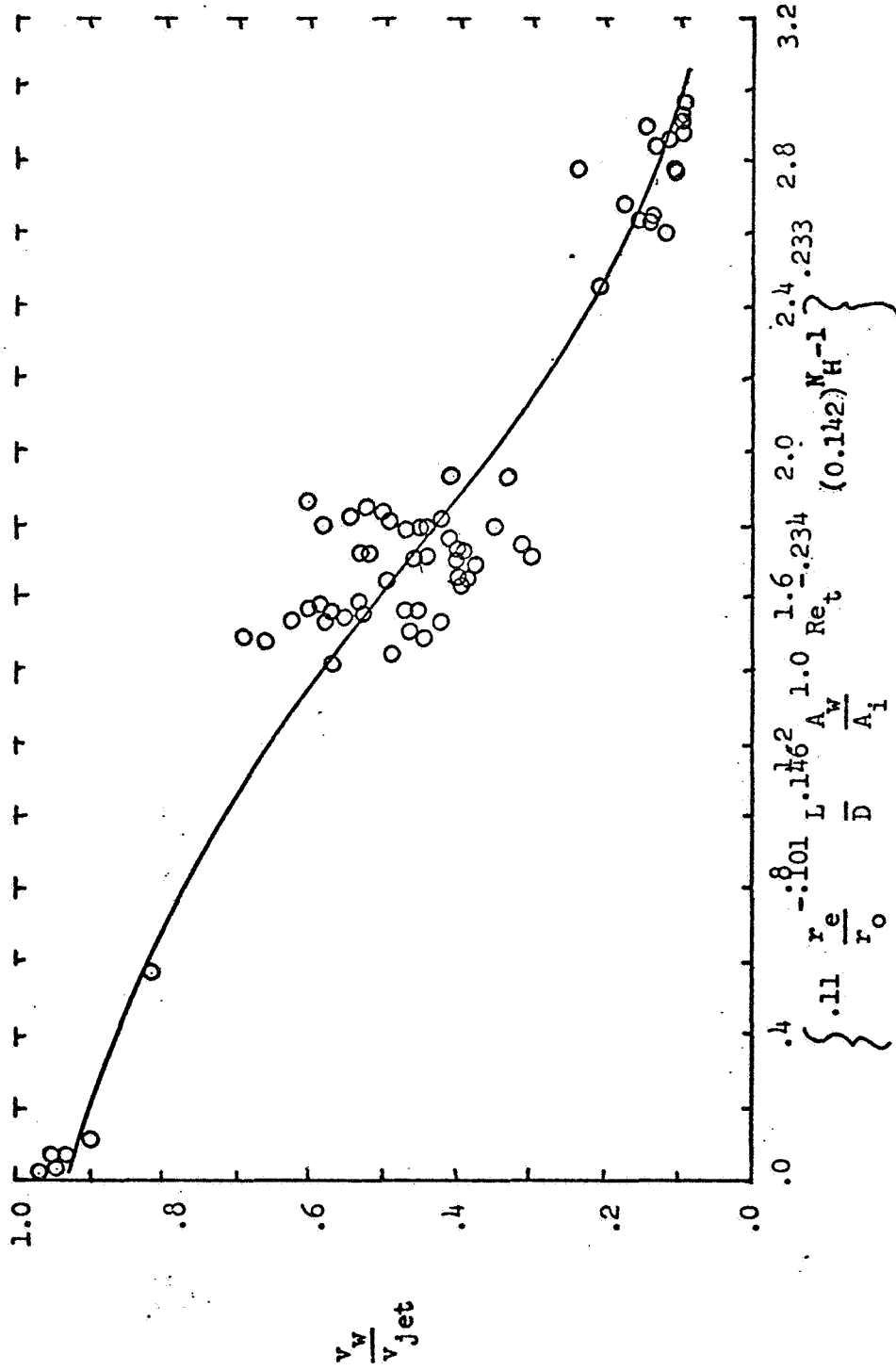


FIG. 3 The recovery factor  $V_w/V_{jet}$  as a function of  $r_e/r_o$ , the ratio of the exhaust hole radius to the outer wall radius;  $L/D$ , the length-to-diameter ratio of the chamber;  $A_w/A_i$ , the ratio of the peripheral wall area to the injection area;  $N_H$ , the number of exhaust holes; and  $Re_t$ , the tangential Reynolds number.

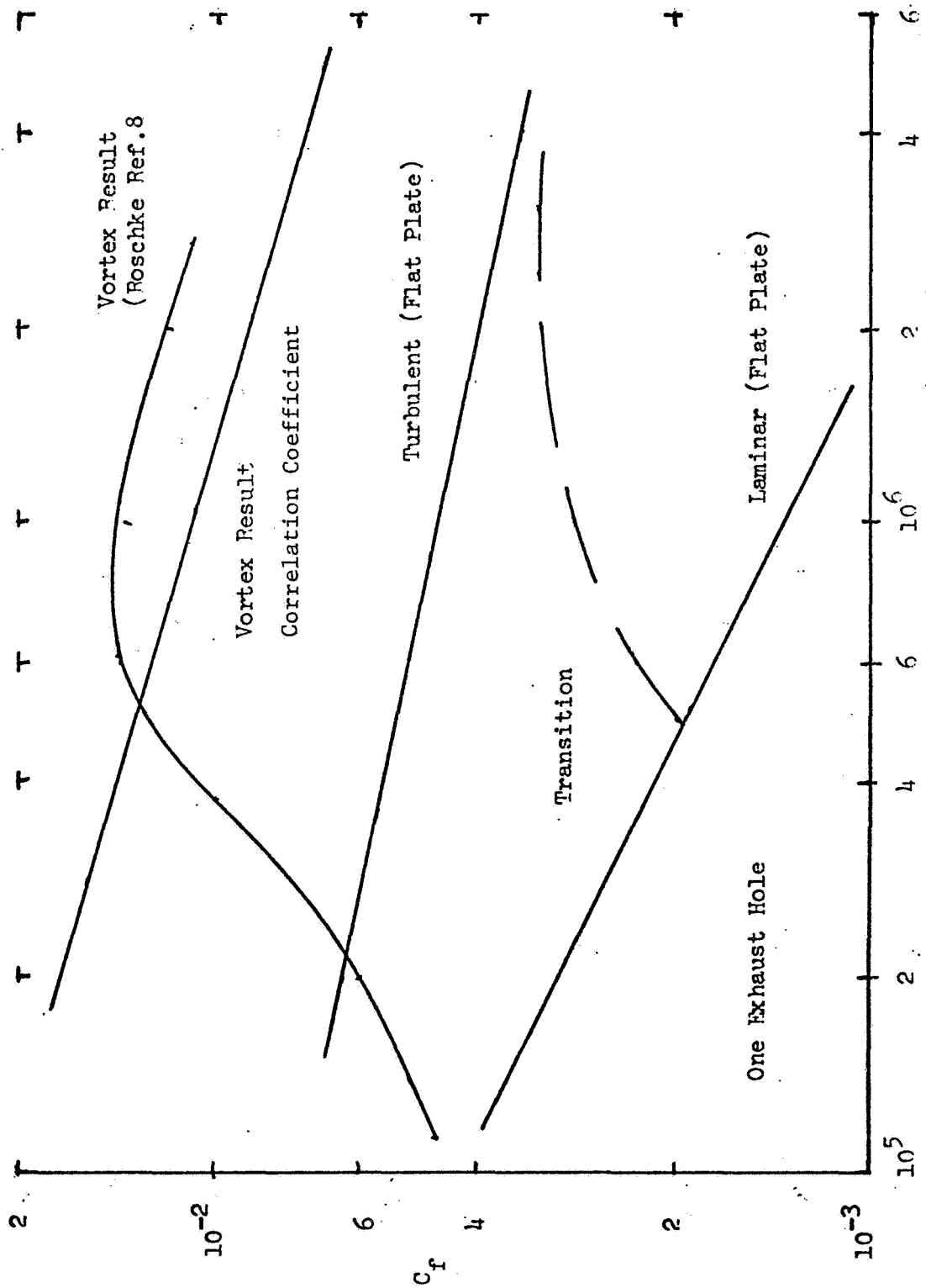


FIG. 4 Comparison of "effective" skin friction coefficient with flat plate results.

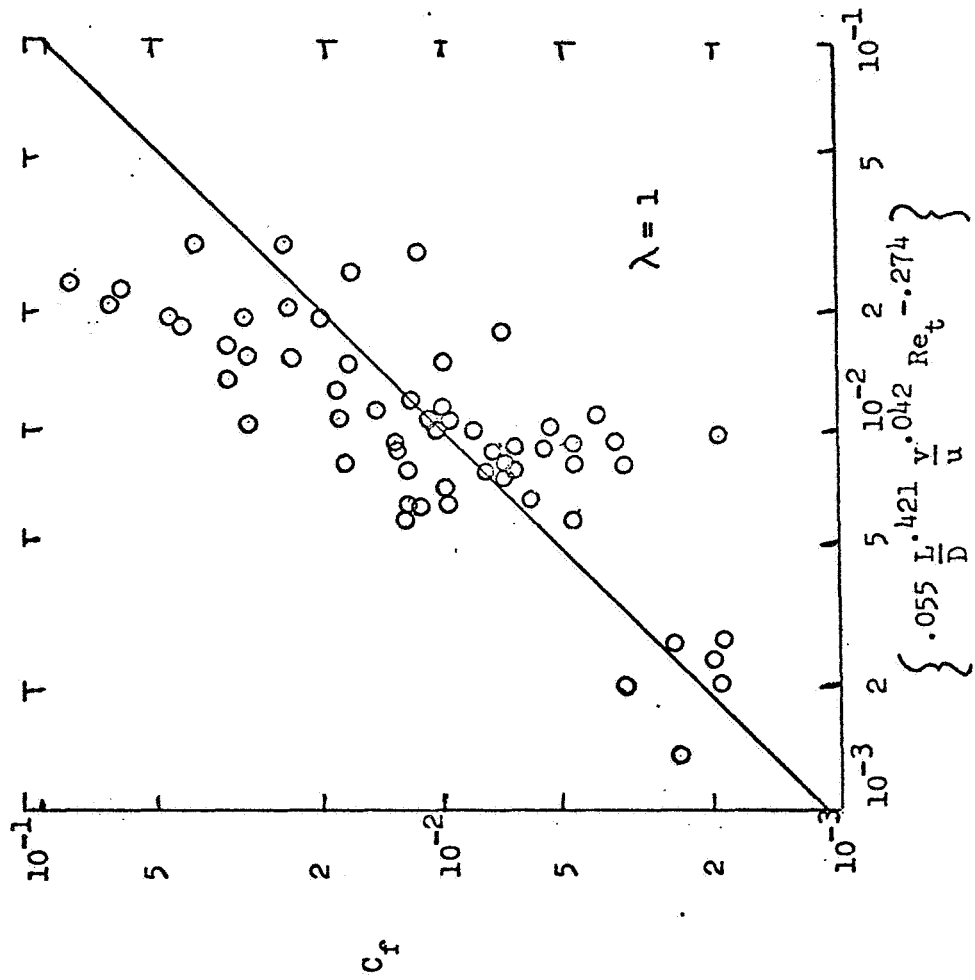


FIG. 5 The variation of the effective end-wall skin friction coefficient with  $L/D$ ,  $v/u$ , and  $Re_t$ .

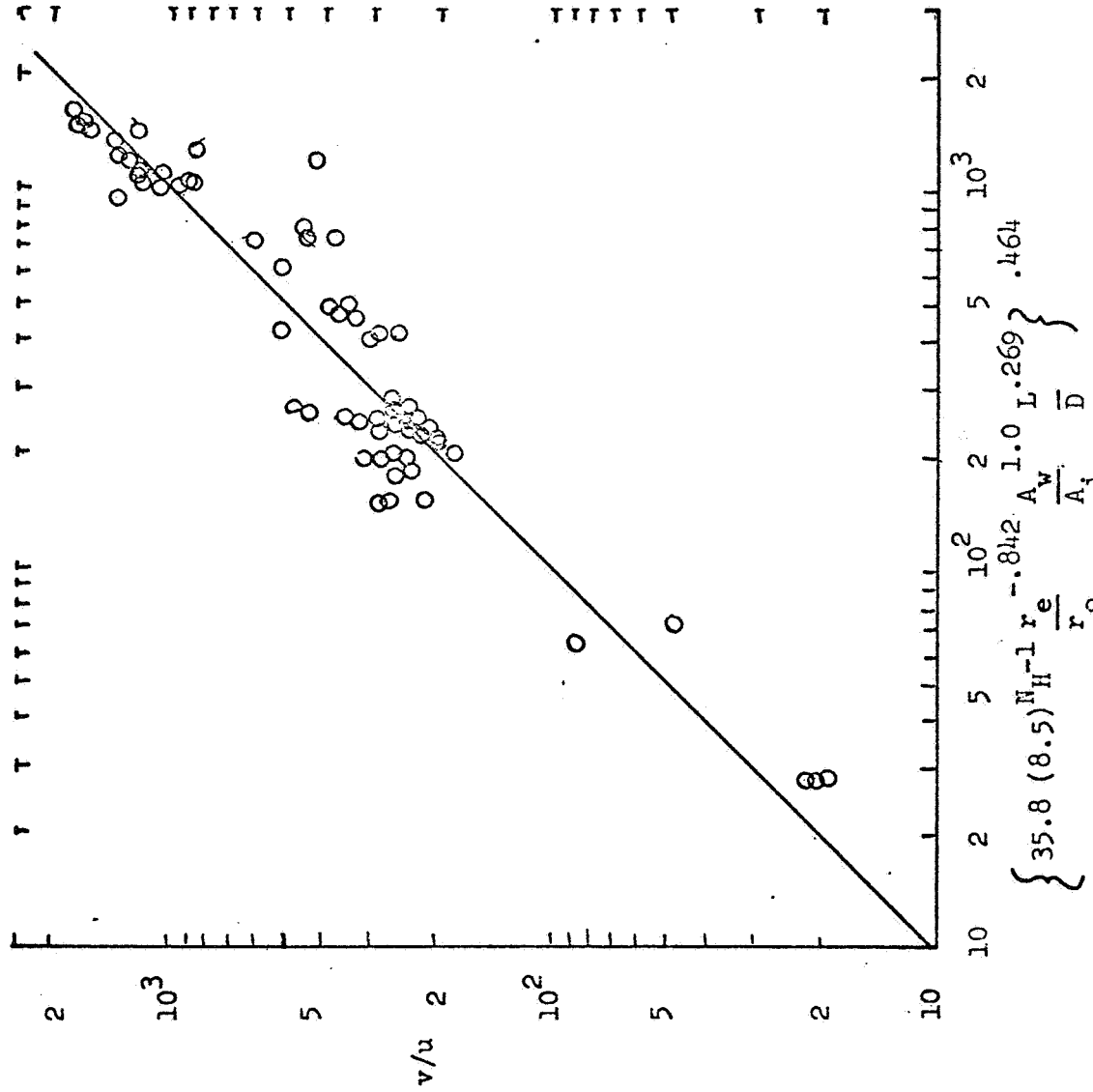


FIG. 6 The velocity ratio as a function of  $r_e/r_o$ ,  $A_w/A_i$ ,  $L/D$ , and  $N_H$ .

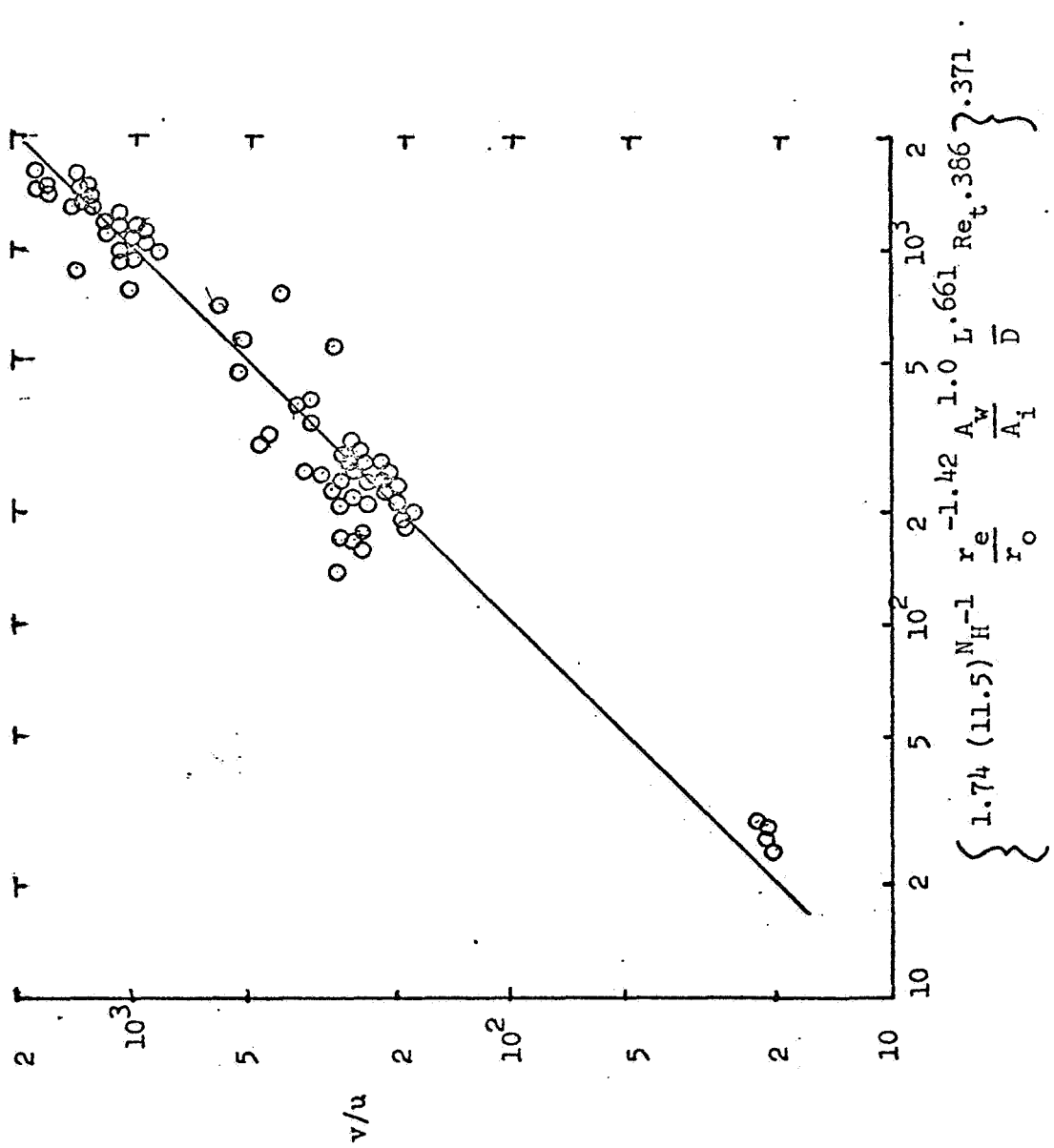


FIG. 7 The velocity ratio as a function of  $r_e/r_o$ ,  $A_w/A_i$ ,  $L/D$ ,  $N_H$ , and  $Re_t$ .

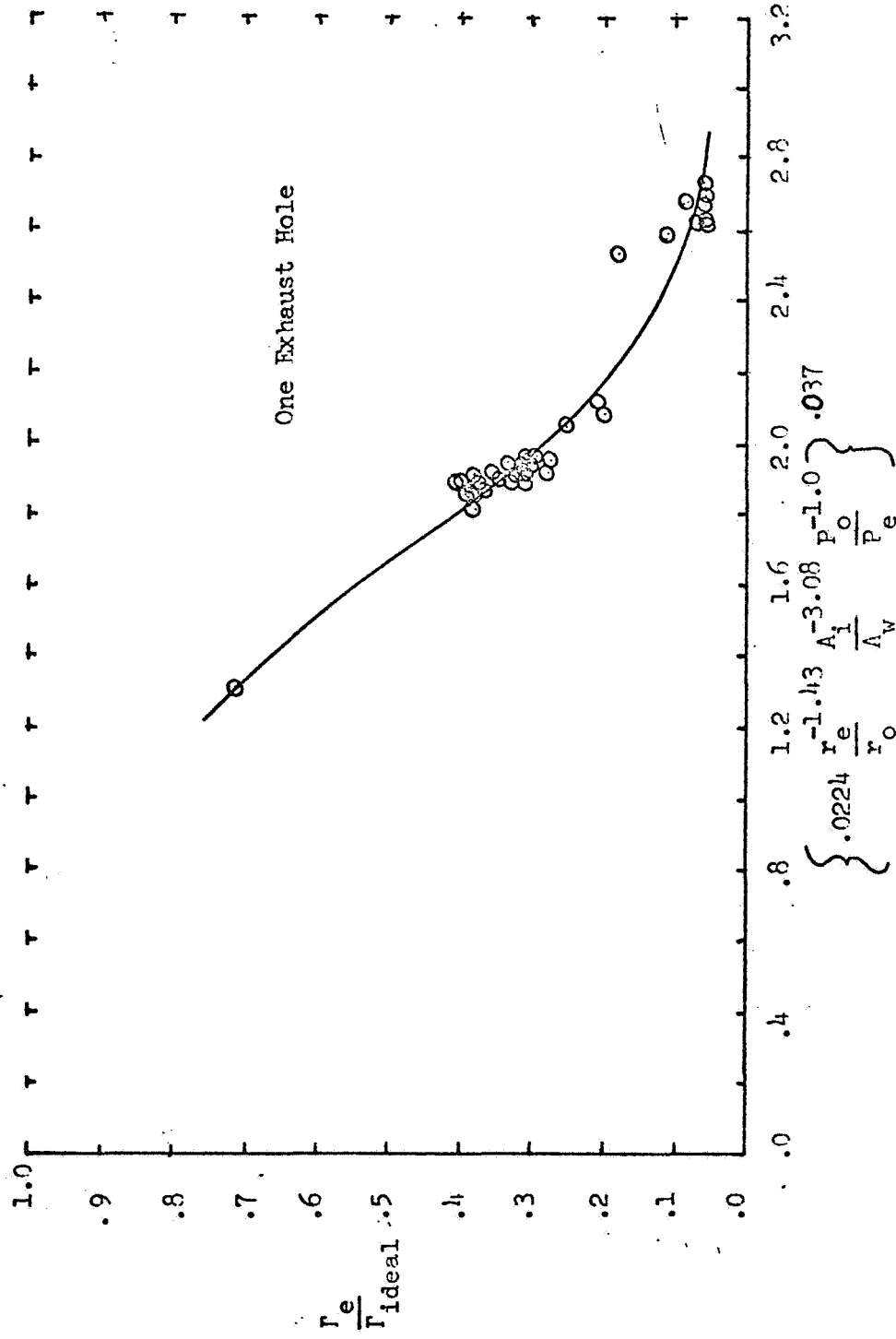


FIG. 8 The ideal circulation ratio as a function of the radius ratio, the wall area ratio, and the pressure ratio.

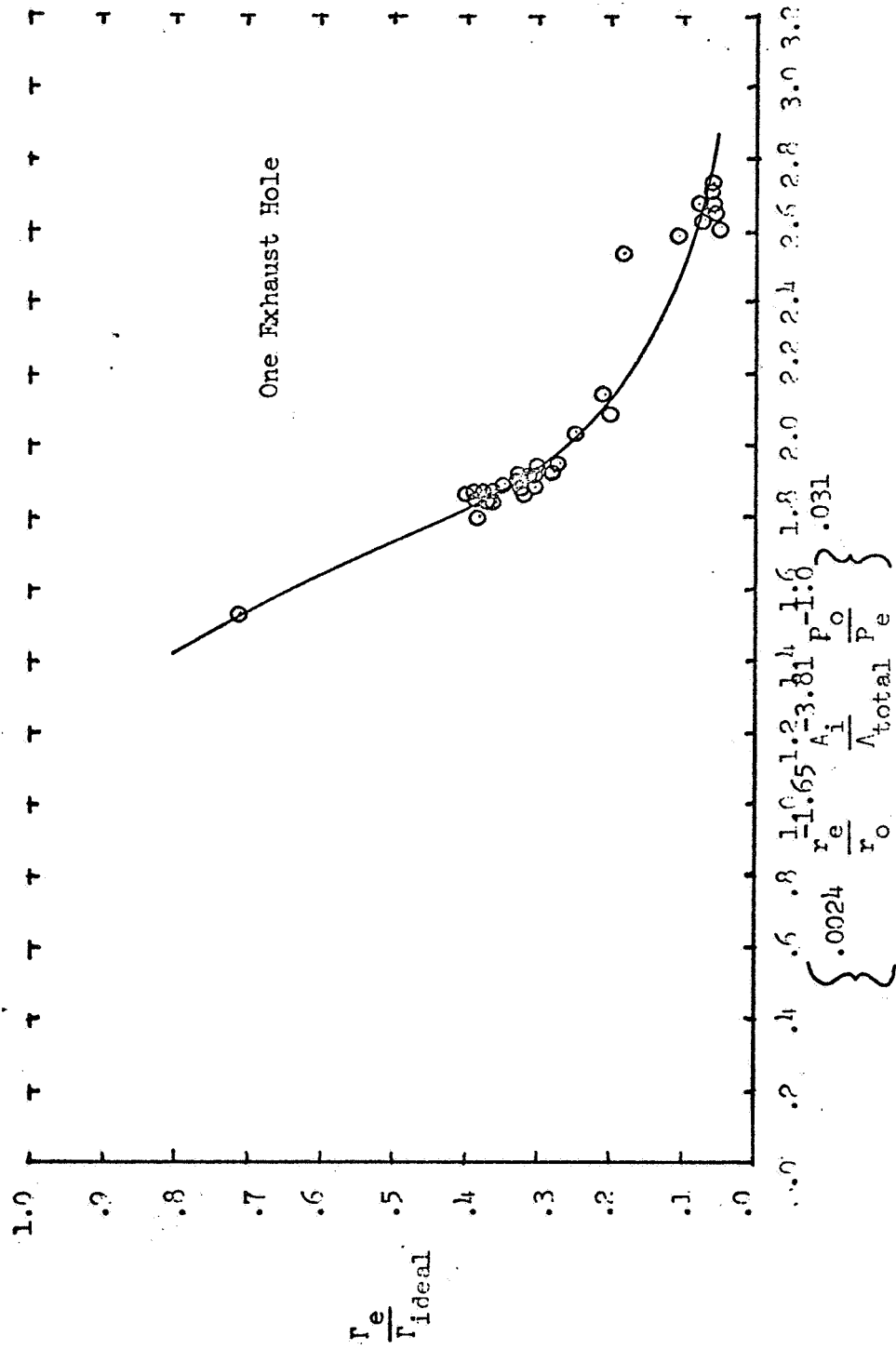


FIG. 9 The ideal circulation ratio as a function of the radius ratio, the total area ratio, and the pressure ratio.

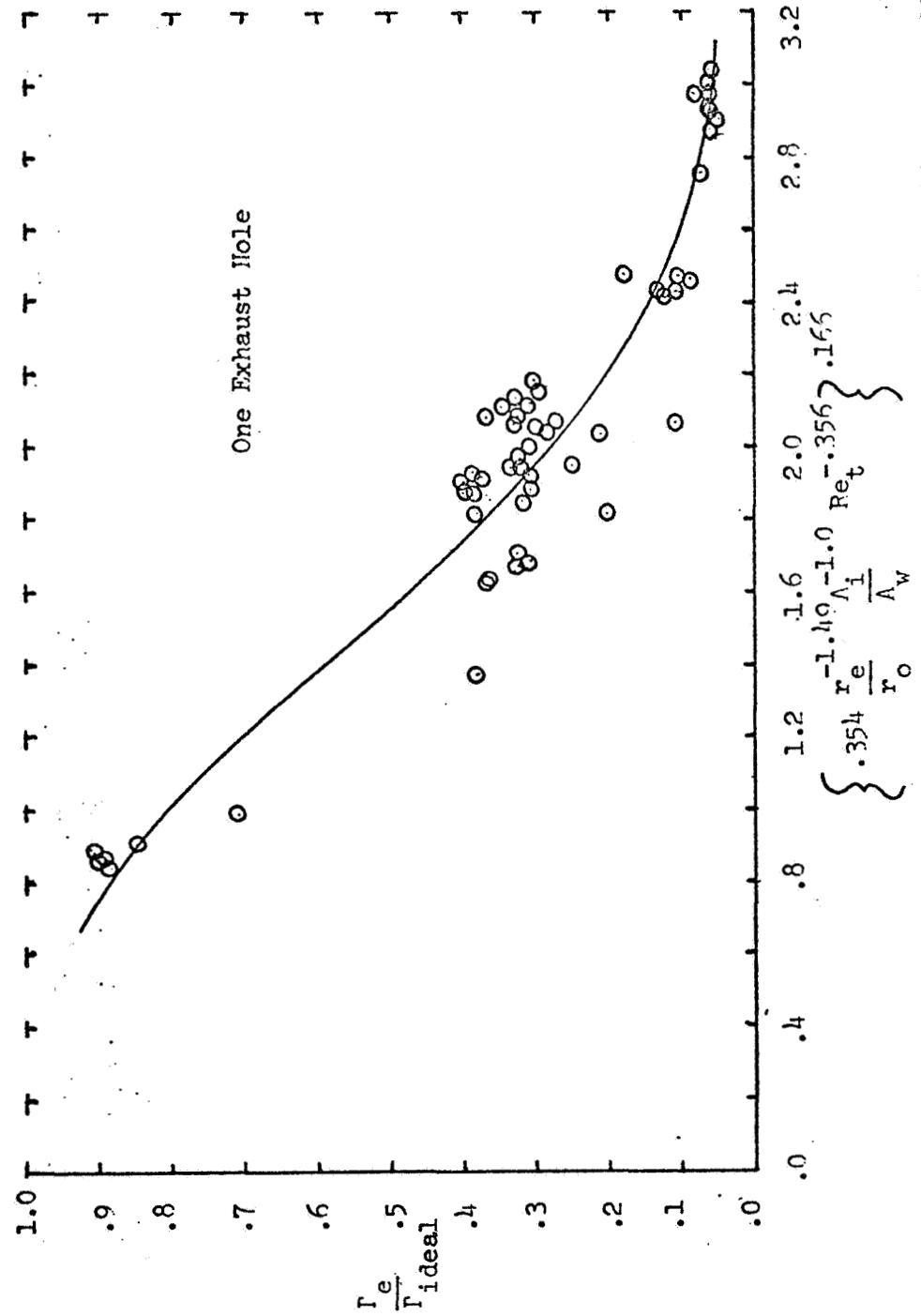


FIG. 10 The ideal circulation ratio as a function of the radius ratio, the wall area ratio, and the tangential Reynolds number.



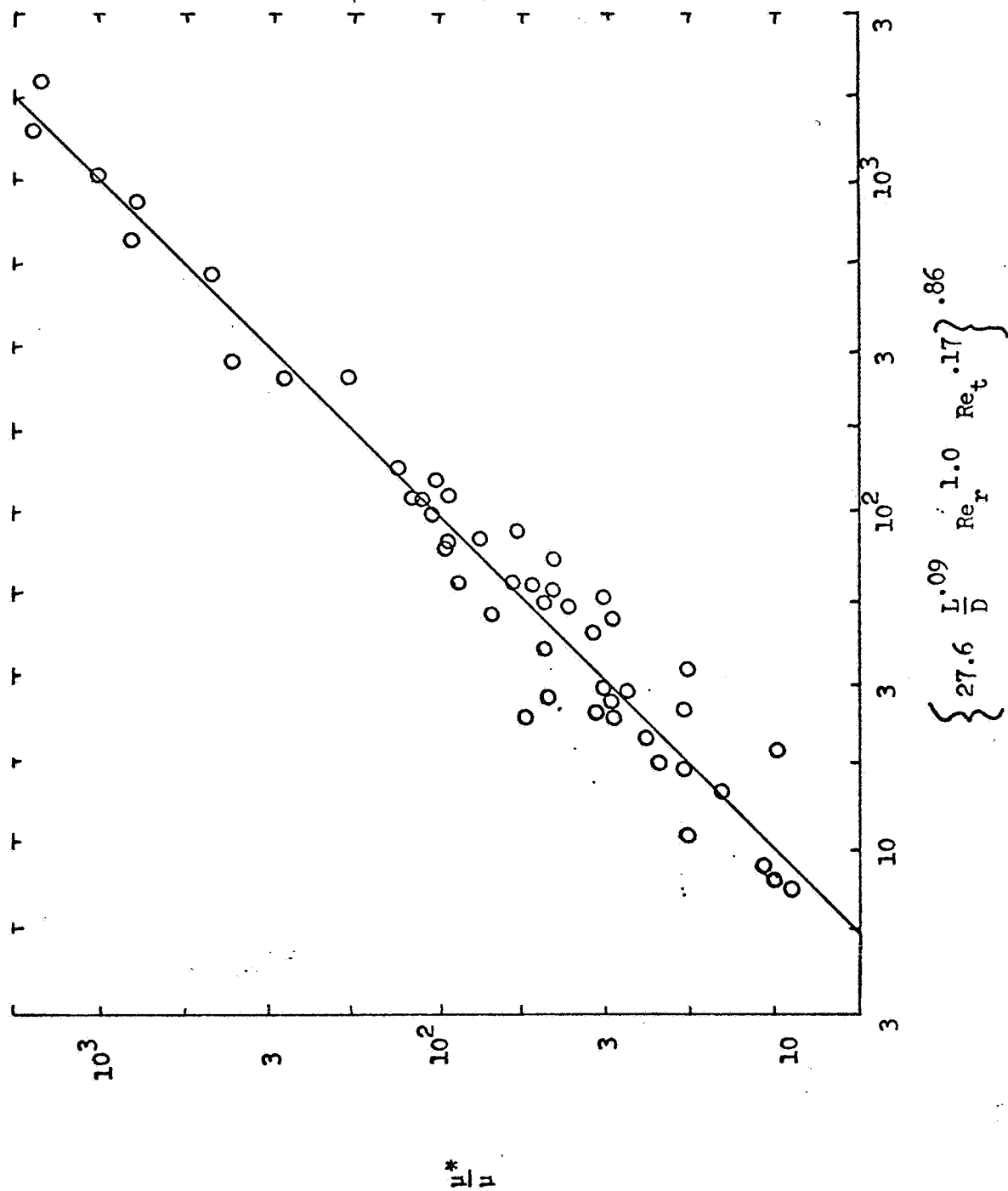


FIG. 12 The ratio of the turbulent "eddy" viscosity to the molecular viscosity as a function of  $L/D, Re_r, Re_t$ .

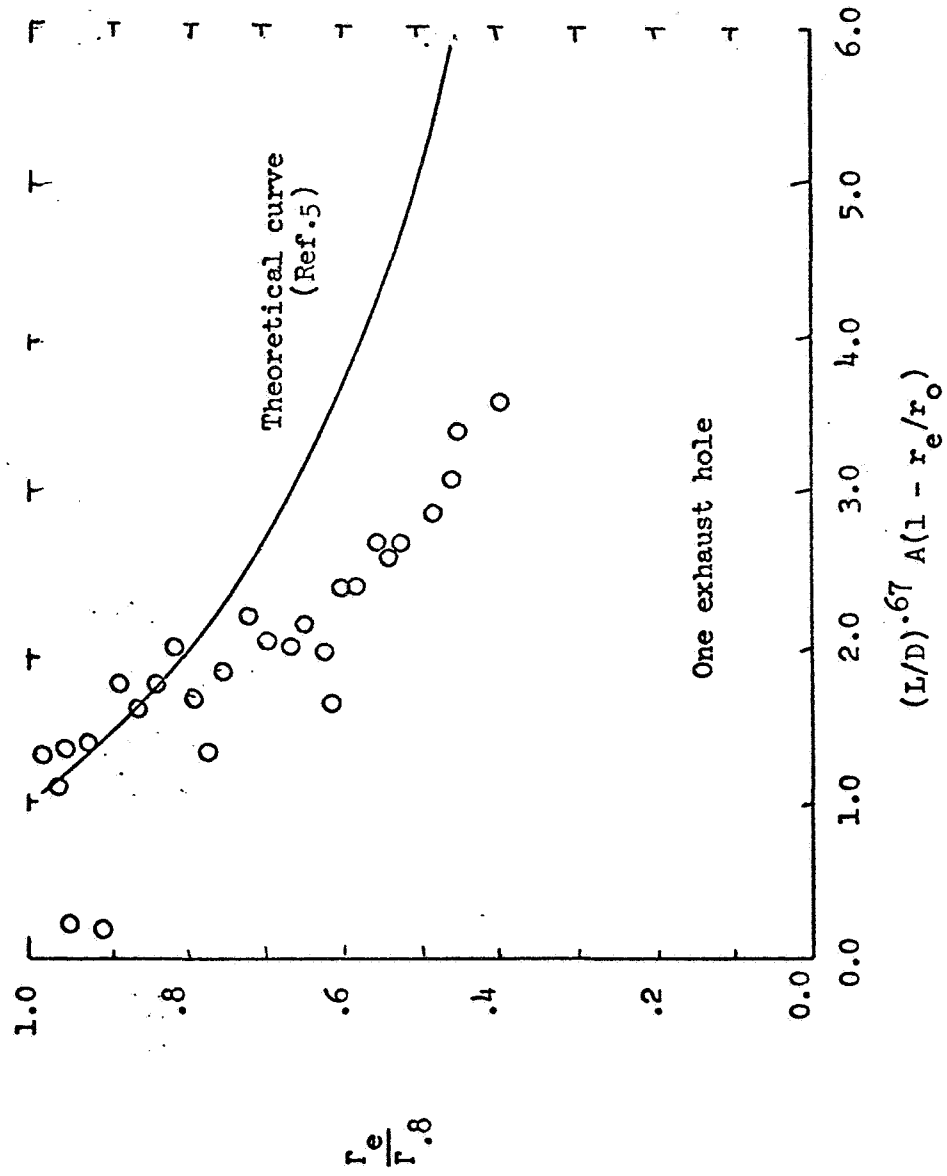


FIG. 11 The circulation ratio as a function of  $L/D$ ,  $r_e/r_o$ , and the boundary layer interaction parameter for incompressible flows.

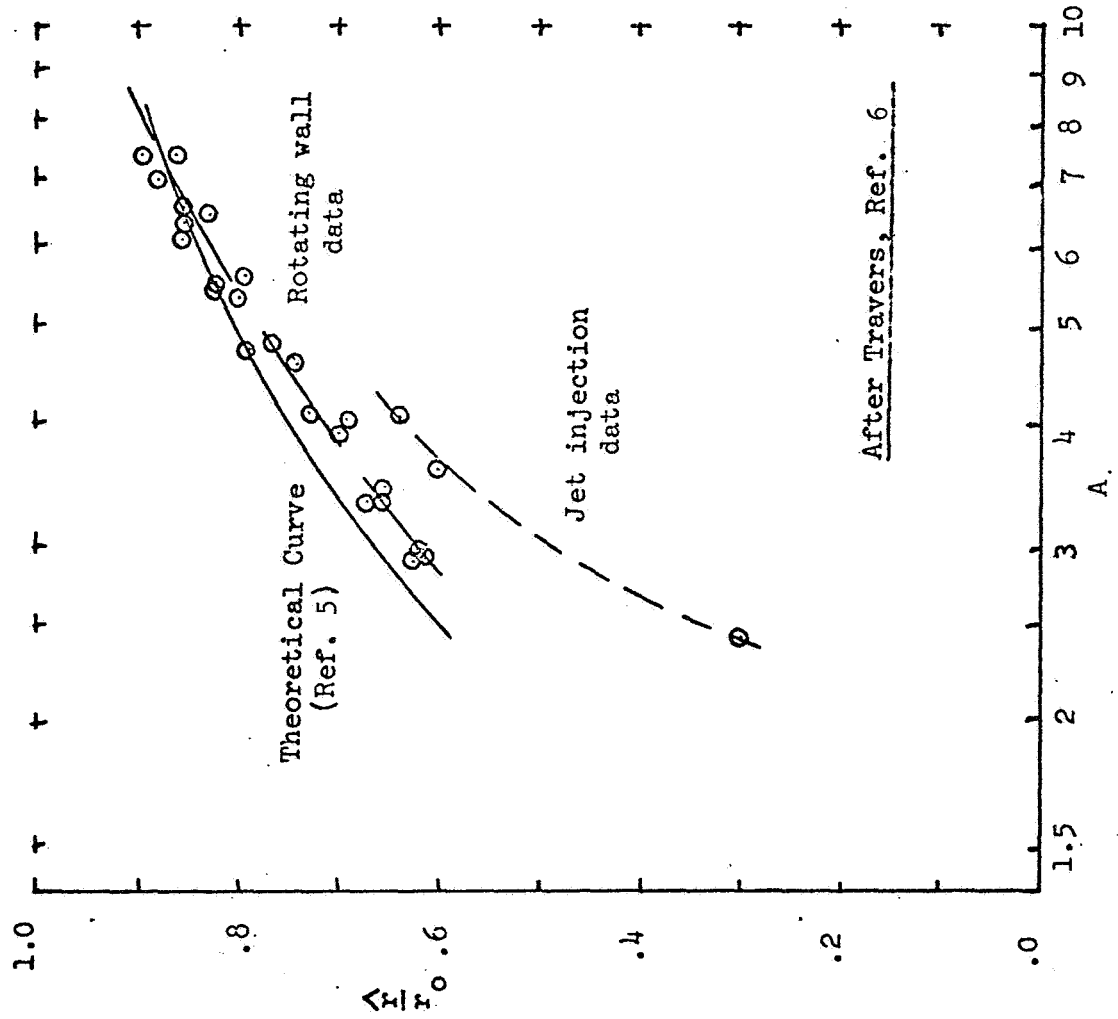


FIG. 13 The normalized radius of stagnation as a function of the boundary-layer interaction parameter ( $A$ ).